

Intermittency in an Optomechanical Cavity Near a Subcritical Hopf Bifurcation

Oren Suchoi, Lior Ella, Oleg Shtempluk, and Eyal Buks
Department of electrical engineering, Technion, Haifa 32000, Israel
(Dated: September 24, 2018)

We experimentally study an optomechanical cavity consisting of an oscillating mechanical resonator embedded in a superconducting microwave transmission line cavity. Tunable optomechanical coupling between the mechanical resonator and the microwave cavity is introduced by positioning a niobium-coated single mode optical fiber above the mechanical resonator. The capacitance between the mechanical resonator and the coated fiber gives rise to optomechanical coupling, which can be controlled by varying the fiber-resonator distance. We study radiation pressure induced self-excited oscillations as a function of microwave driving parameters (frequency and power). Intermittency between limit cycle and steady state behaviors is observed with blue-detuned driving frequency. The experimental results are accounted for by a model that takes into account the Duffing-like nonlinearity of the microwave cavity. A stability analysis reveals a subcritical Hopf bifurcation near the region where intermittency is observed.

PACS numbers: 46.40.-f, 05.45.-a, 65.40.De, 62.40.+i

The field of cavity optomechanics [10, 28, 44, 51] deals with a family of systems, each is composed of two coupled elements. The first one is a mechanical resonator, commonly having low damping rate, and the second one is an electromagnetic cavity, which is typically externally driven. Both radiation pressure [2, 13, 19, 27, 37, 57, 72, 73, 79] and bolometric force [4, 39, 47, 50, 52, 54, 55, 61, 67, 86, 88] can give rise to the coupling between the mechanical resonator and the cavity. In recent years a variety of cavity optomechanical systems have been constructed and studied [2, 14, 16, 19, 20, 27, 29, 31, 35, 44, 45, 55, 58, 66, 72, 75, 76, 79], and phenomena such as mode cooling [16, 30, 71, 75, 76], self-excited oscillations [4, 14, 15, 21, 31, 42, 52, 54, 66] and optically induced transparency [40, 59, 70, 82] have been investigated. In addition to applications in metrology [9, 18] and photonics [5, 34, 89], the appeal of optomechanics lies in the potential for observation of macroscopic quantum behavior in mechanical systems [6, 23, 25, 26, 32, 41, 43, 48, 53, 58, 60, 62, 63, 65, 68, 76, 77, 80, 81, 83, 84]. While much experimental and theoretical progress has been made in reaching the ground state and observing the linear dynamics of mechanical objects, it is becoming appreciated that nonlinearity allows the creation of non-classical mechanical states [49] and can be exploited for improving the efficiency of optomechanical cooling [56]. It is therefore important to study and shed light on the nonlinear dynamics of these devices.

In this work we experimentally study self-excited oscillations in an optomechanical cavity operating in the microwave band. We introduce a novel method for achieving strong and tunable optomechanical coupling, which is based on positioning a metallically coated optical fiber near the mechanical resonator. The microwave cavity, which is made of a superconducting aluminum microstrip, exhibits Kerr type nonlinearity [11, 22, 74, 85], which significantly affects the dynamics of the entire op-

tomechanical system [56]. We study the dependence of the self-excited oscillations on the driving parameters of the cavity and found that a good agreement with theory can be obtained provided that cavity nonlinearity is taken into account [56]. We experimentally find that in a certain region of drive parameters the system exhibits random jumps between a limit-cycle (i.e. self-excited oscillations) and a steady-state. A theoretical stability analysis reveals that this observed intermittency behavior occurs near a subcritical [7, 33, 46, 53] Hopf bifurcation [48, 80].

The experimental setup is schematically depicted in Fig. 1. Magnetron DC sputtering is employed for coating a high resistivity silicon wafer with aluminum. The aluminum layer is annealed *in situ* at 400°C for 10 – 30 minutes to reduce internal stress in the layer [36]. A standard photo-lithography process is used to pattern the microwave microstrip cavity. At the open end of the microstrip a 100nm thick SiN membrane is fabricated [88]. The mechanical resonator is made by releasing a $100 \times 100 \mu\text{m}^2$ trampoline supported by four beams using electron cyclotron resonance (ECR) dry etch. At the other end the cavity is weakly coupled to a feed-line, which guides both the injected and reflected microwave signals. The results presented here are obtained with a device having a fundamental cavity resonance frequency $\omega_a/2\pi = 2.5465$ GHz, cavity linear damping rate $\gamma_a/2\pi = 420$ kHz, fundamental mechanical resonance frequency $\omega_b/2\pi = 12.1$ kHz and mechanical Q-factor $Q_b = 3700$.

As can be seen in Fig. 1, a single mode optical fiber coated with niobium is placed above the suspended trampoline. In the presence of the coated fiber two optomechanical cavities are formed, one in the microwave band and the other in the optical band [87]. The fact that both optomechanical cavities share the same mechanical resonator can be exploited for conversion between microwave and optical photons [1, 8, 17, 24, 38]. However, in the present work we employ the optical cavity and the

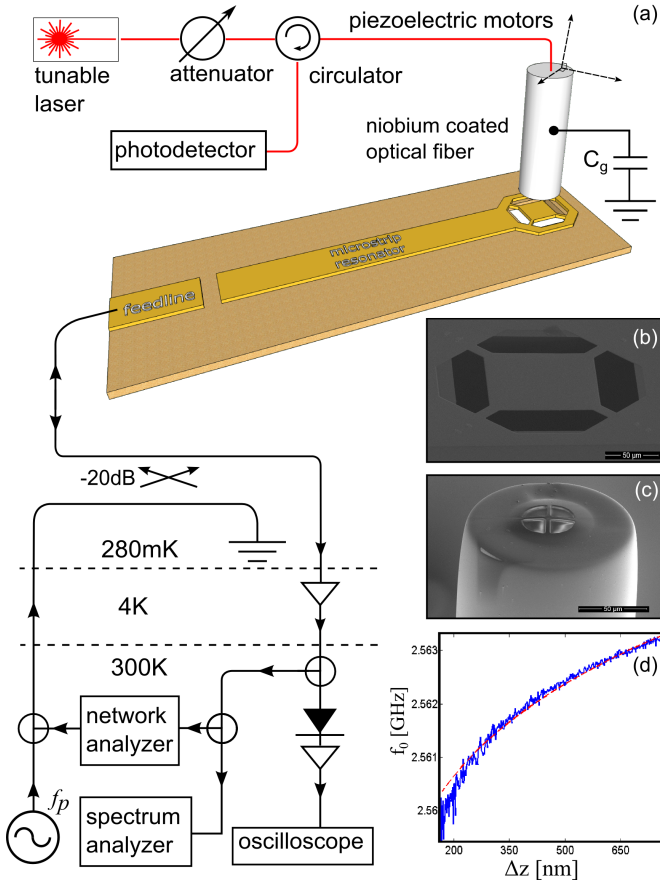


FIG. 1: Experimental Setup (color online). The Microwave cavity is a microstrip made of aluminum over high resistivity silicon wafer coated with a 100 nm thick SiN layer. The mechanical resonator at the end of the microstrip is a suspended trampoline supported by four beams. Electron micrograph of the trampoline is shown in panel (b). The optomechanical coupling is generated using a niobium coated optical fiber that is positioned at sub-micron distance from the trampoline. Several windows are opened in the niobium layer on the fiber tip using FIB, as can be seen in panel (c). The optical setup (seen above the sample) allows using the optical fiber for displacement detection, whereas the microwave setup (seen below the sample) is employed for measuring the cavity response. The coated fiber is galvanically connected to both AC and DC voltage sources with a bias-T (not seen in the sketch), which can be used to externally actuate the mechanical resonator. The sample is mounted inside a closed copper package, which is internally coated with niobium. Measurements are performed in a dilution refrigerator operating at a temperature of 0.28 K and in vacuum. Panel (d) shows the measured (solid) and calculated (dashed) cavity resonance frequency f_0 vs. fiber-trampoline distance Δz .

optical setup seen in Fig. 1 only for fiber positioning and for characterization of the mechanical resonator at high temperatures, whereas all low temperature measurements that are discussed below are done in the microwave band only.

We employ a telecom single mode optical fiber having a fiber Bragg grating (FBG) mirror [87] and a focusing lens, made by melting the fiber tip. Magnetron DC sputtering is used for coating the fiber with niobium. To allow optical transmission, we etch the niobium coating using focused ion beam (FIB), exposing thus the core of the fiber at the tip. A cryogenic piezoelectric 3-axis positioning system having sub-nanometer resolution is employed for manipulating the position of the optical fiber.

Optomechanical coupling between the microwave cavity and the mechanical resonator is introduced due to the capacitance between the coated fiber and the suspended trampoline, which is given by approximately $C_{SP} = 2\pi\epsilon_0 R_F \log(R_F/\Delta z)$ [69], where $R_F = 350 \mu\text{m}$ is the radius of curvature of the melted fiber tip, Δz is the fiber-trampoline distance and ϵ_0 is the vacuum permittivity. A hole of diameter $d_H = 2.4\text{mm}$ and depth $h_H = 2.7\text{mm}$ is drilled in the sample package, which is made of copper, above the trampoline in order to allow inserting the optical fiber, which has an outer diameter of $d_F = 125 \mu\text{m}$. When the fiber is centered inside the hole, the fiber-package coaxial capacitance is given by $C_g = 2\pi\epsilon_0 h_H / \log(d_H/d_F)$ [64]. When radiation loss is disregarded, the effect of the coated fiber on microwave cavity modes can be accounted for by assuming that a termination having purely imaginary impedance given by $Z_T = 1/i\omega C$, where $C^{-1} = C_{SP}^{-1} + C_g^{-1}$, has been introduced between the microstrip end and ground. The frequencies f_a of the cavity modes can be found by solving $\tan(\kappa l_M) = iZ_0/Z_T$ [64], where the propagation constant κ is related to f_a by $f_a = \kappa c'/2\pi$, c' is the propagation velocity in the microstrip, l_M is the length of the microstrip, and $Z_0 = 48 \Omega$ is its characteristic impedance. Comparison between the measured and calculated values of the cavity fundamental mode frequency f_0 is seen in panel (d) of Fig. 1. The dependence of f_0 on fiber-trampoline distance Δz allows the extraction of optomechanical coupling coefficient Ω , which is found to be given by $\Omega/x_{b0} = 55\text{MHz } \mu\text{m}^{-1}$ for our chosen operating point, where $x_{b0} = \sqrt{\hbar/2m\omega_b} = 1.1 \times 10^{-8} \mu\text{m}$ is the mechanical zero point amplitude, and where $m = 5.4 \times 10^{-12}\text{kg}$ is the effective mass of the mechanical mode.

The microwave cavity is excited by injecting a monochromatic pump signal having frequency $f_p = \omega_p/2\pi$ and amplitude b_p into the feedline and monitoring the off-reflected signal using either a spectrum analyzer or a diode connected to an oscilloscope [see panel (a) of Fig. 1]. The amplitude b_p is related to the pump power P_p by $P_p = \hbar\omega_a |b_p|^2 / 2\gamma_{a1}$, where γ_{a1} represents the contribution to the total cavity linear damping rate γ_a due to cavity-feedline coupling [85]. In the absence of any optomechanical coupling (i.e. when the fiber is positioned far from the trampoline) the cavity reflectivity exhibits bistability in a certain region in the plane of pump parameters (frequency f_p and amplitude b_p) originates by cavity Kerr nonlinearity. The border line of this region

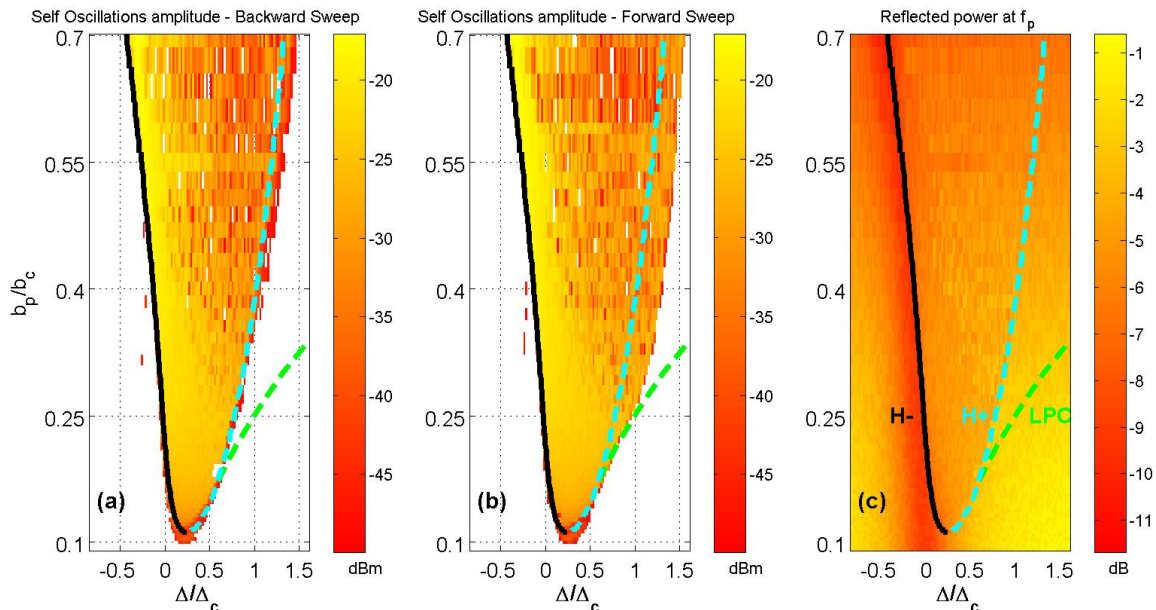


FIG. 2: Self-Excited Oscillations (color online). Panels (a) and (b) show the reflected power at angular frequency $\omega_p - \omega_b$ for backward and forward frequency sweeps, respectively. The pump critical power is $P_c = -19.5$ dBm and the pump critical detuning is $\Delta_c = -2\pi \times 0.7$ MHz. Panel (c) shows the reflected power at angular frequency ω_p . Note the pulling in the frequency response due to the cavity Kerr nonlinearity. The solid black, dotted cyan and dotted green lines represent, respectively, supercritical Hopf, subcritical Hopf and limit point of cycle bifurcations. The following cavity parameters are employed for the bifurcation calculation $K_a/\omega_a = -1.44 \times 10^{-15}$ and $\gamma_{a3}/K_a = 0.04$.

contains a cusp point, which is also known as the onset of bistability point [85]. The values of pump frequency and pump amplitude at that critical point are labeled by $f_c = \omega_c/2\pi$ and b_c , respectively. In what follows we employ normalized and dimensionless parameters for the pump detuning $\Delta/\Delta_c = (\omega_p - \omega_a)/|\omega_c - \omega_a|$ and for the pump amplitude b_p/b_c .

Panels (a) and (b) of Fig. 2 show the reflected microwave power, which is measured using a spectrum analyzer, at frequency $f_p - f_b$, where $f_b = \omega_b/2\pi$ is the mechanical resonance frequency, for both forward and backward sweeps of the pump frequency f_p . A strong peak is found at frequency $f_p - f_b$ [as well as at other harmonics $f_p + n f_b$, where n is integer, as can be seen in panel (a) of Fig. 3] in a certain region in the plane of normalized pump parameters Δ/Δ_c and b_p/b_c , inside which self-excited oscillations occur. The height of the peak at frequency $f_p - f_b$ is plotted in panels (a) and (b) of Fig. 2. The results obtained with backward sweep [panel (a)] differ from those obtained with forward sweep [panel (b)], which indicates that the cavity response is hysteretic due to bistability. Panel (c) depicts the reflected power at f_p .

Cavity nonlinearity plays a crucial role in the observed behavior of the system. We employ the theoretical modeling of Refs. [12, 56] to account for cavity Kerr nonlinearity [22, 78]. The equations of motion in the rotating frame of the cavity for the annihilation operators A_a and A_b of the cavity and mechanical resonator, respec-

tively, are found to be given by $dA_a/dt + \Theta_a = F_a$ and $dA_b/dt + \Theta_b = F_b$ where

$$\Theta_a = [i\Delta_a^{\text{eff}} + \gamma_a + (iK_a + \gamma_{a3})N_a] A_a + b_p, \quad (1)$$

$$\Theta_b = (i\omega_b + \gamma_b) A_b + i\Omega N_a, \quad (2)$$

and where $\Delta_a^{\text{eff}} = \omega_a - \omega_p + \Omega(A_b + A_b^\dagger)$ is the effective cavity detuning, Ω is the optomechanical coupling coefficient, K_a is the cavity Kerr nonlinearity constant, ω_a (ω_b) is the cavity (mechanical) angular resonance frequency, γ_a (γ_b) is the cavity (mechanical) linear damping rate, γ_{a3} is the cavity nonlinear damping rate, $N_a = A_a^\dagger A_a$ is the cavity number operator and b_p is the pump amplitude. The terms F_a and F_b represent white noise having (frequency independent) power spectrum given by $S_a = 2\Gamma_a(1 - e^{-\beta\hbar\omega_a})^{-1}$ and $S_b = 2\gamma_b(1 - e^{-\beta\hbar\omega_b})^{-1}$, respectively, where $\Gamma_a = \gamma_a + 2\gamma_{a3}\langle N_a \rangle$, $\beta = 1/k_B T$, k_B is Boltzmann's constant and T is the temperature.

The stability map of the system is obtained using the numerical continuation package MATCONT (URL: <http://www.matcont.ugent.be/>). First, a steady state solution (i.e. solution to $\Theta_a = \Theta_b = 0$) is found for each operating point in the plane of pump parameters. Note that for the region seen in Fig. 2 the steady state is unique (since $b_p/b_c < 1$). Then MATCONT is employed to identify bifurcations. The solid black, dotted cyan and

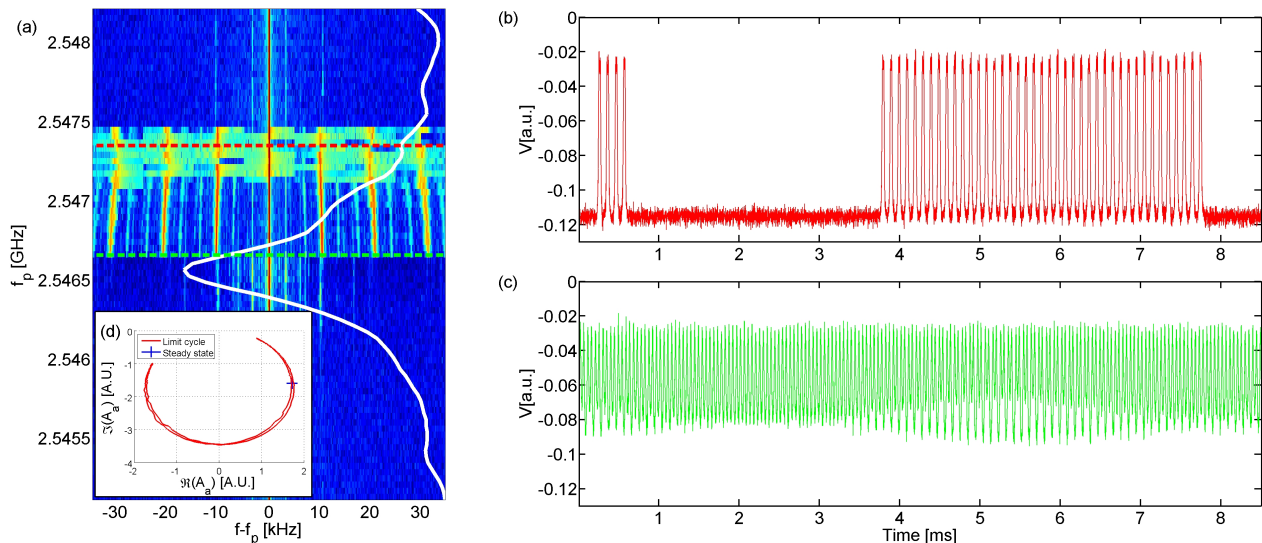


FIG. 3: Intermittency (color online). The measurement of the reflected signal using a spectrum analyzer is seen in panel (a), whereas the time traces seen in panels (b) and (c) are measured using an oscilloscope for two values of f_p , which are indicated in panel (a) by the two dotted lines. The solid white line in panel (a) shows the reflected power at the pump frequency f_p . Noise-induced transitions between limit-cycle and steady state are seen in panel (b). Panel (d) shows the projection of the limit cycle (red line) and steady state (blue cross) on the complex A_a plane.

dotted green lines in Fig. 2 represent, respectively, supercritical Hopf (labeled as H_-), subcritical Hopf (labeled as H_+) and limit point of cycle (LPC) bifurcations. In the numerical investigation noise is disregarded and the operators A_a and A_b are treated as c -numbers. The cavity parameters that are used for the numerical calculation are listed in the caption of Fig. 2. The bifurcation lines divide the region in the plane of pump parameters seen in Fig. 2 into three zones. In the zone between the H_- and H_+ bifurcations only a single limit-cycle is found to be locally stable (though the existence of other locally stable solutions cannot be ruled out), in the zone between the H_+ and LPC bifurcations bistability of a limit-cycle and a steady state occurs, whereas elsewhere only a unique steady state is found.

Intermittency, i.e. random jumps between the limit-cycle and the steady state, is experimentally observed for $b_p/b_c > 0.2$. Fig. 3 shows frequency and time domain measurements taken with normalized pump amplitude given by $b_p/b_c = 0.58$. Panel (a) shows the frequency decomposition of the reflected signal as the pump frequency f_p is scanned and the white line shows the reflected power at frequency f_p . Regular self-excited oscillations in the time domain can be seen in panel (c) for normalized detuning $\Delta/\Delta_c = 0.2$. At larger detuning $\Delta/\Delta_c = 1.5$ (in the bistable zone), however, random transitions between the limit cycle and the steady state occur, as can be seen in panel (b). The limit cycle and the steady state in the complex A_a projection plane of phase space are plotted in panel (d). Note that the dynamics near

the steady state remains relatively slow even when it becomes locally unstable (i.e. in the zone between the H_- and H_+ bifurcations). Consequently, in the presence of noise even a locally unstable steady state can give rise to intermittency-like behavior provided that it is sufficiently close to the limit cycle. Indeed, intermittency is experimentally observed on both sides of the H_+ bifurcation.

In summary, we find that a subcritical Hopf bifurcation is the underlying mechanism that is responsible for the experimentally observed intermittency. While the current study is focused on the classical dynamics, future study will explore the possibility of exploiting dynamical bistability for the creation of macroscopic non-classical states of the optomechanical system [3].

This work was supported by the Israel Science Foundation, the bi-national science foundation, the Deborah Foundation, the Israel Ministry of Science, the Russell Berrie Nanotechnology Institute, the European STREP QNEMS Project and MAFAT. The authors thank Ya'akov Schneider for helping in sample fabrication.

-
- [1] Andrews, R., R. Peterson, T. Purdy, K. Cicak, R. Simmonds, C. Regal, and K. Lehnert, 2013, arXiv preprint arXiv:1310.5276 .
 - [2] Arcizet, O., P.-F. Cohadon, T. Briant, M. Pinard, and A. Heidmann, 2006, Nature **444**, 71.
 - [3] Armour, A. D., and D. A. Rodrigues, 2012, Comptes Rendus Physique **13**(5), 440.

- [4] Aubin, K., M. Zalalutdinov, T. Alan, R. Reichenbach, R. Rand, A. Zehnder, J. Parpia, and H. Craighead, 2004, *J. MEMS* **13**, 1018.
- [5] Bagheri, M., M. Poot, M. Li, W. P. H. Pernice, and H. X. Tang, 2011, *Nature Nanotechnology* **6**, 726.
- [6] Bahrami, M., M. Paternostro, A. Bassi, and H. Ulbricht, 2014, arXiv:1402.5421 .
- [7] Blocher, D., R. H. Rand, and A. T. Zehnder, 2013, *International Journal of Non-Linear Mechanics* **52**, 119.
- [8] Bochmann, J., A. Vainsencher, D. D. Awschalom, and A. N. Cleland, 2013, *Nature Physics* **103**, 122602.
- [9] Braginsky, V., and F. Khalili, 1995, *Quantum Measurement* (Cambridge University Press, Cambridge).
- [10] Braginsky, V., and A. Manukin, 1967, *Soviet Physics JETP* **25**, 653.
- [11] Brkje, K., A. Nunnenkamp, J. D. Teufel, and S. M. Girvin, 2013, *Phys. Rev. Lett.* **111**, 053603, URL <http://link.aps.org/doi/10.1103/PhysRevLett.111.053603>.
- [12] Buks, E., 2012, *C. R. Physique* **13**, 454.
- [13] Carmon, T., H. Rokhsari, L. Yang, T. J. Kippenberg, and K. J. Vahala, 2005, *Phys. Rev. Lett.* **94**, 223902.
- [14] Carmon, T., H. Rokhsari, L. Yang, T. J. Kippenberg, and K. J. Vahala, 2005, *Phys. Rev. Lett.* **94**, 223902.
- [15] Carmon, T., and K. J. Vahala, 2007, *Phys. Rev. Lett.* **98**, 123901.
- [16] Chan, J., T. Alegre, A. Safavi-Naeini, J. Hill, A. Krause, S. Gröblacher, M. Aspelmeyer, and O. Painter, 2011, *Nature* **478**(7367), 89.
- [17] Clader, B., 2014, arXiv:1403.7056 .
- [18] Clerk, A., M. Devoret, S. Girvin, F. Marquardt, and R. Schoelkopf, 2010, *Reviews of Modern Physics* **82**(2), 1155.
- [19] Corbitt, T., Y. Chen, E. Innerhofer, H. Müller-Ebhardt, D. Ottaway, H. Rehbein, D. Sigg, S. Whitcomb, C. Wipf, and N. Mavalvala, 2007, *Physical review letters* **98**(15), 150802.
- [20] Corbitt, T., and N. Mavalvala, 2004, *Journal of Optics B: Quantum and Semiclassical Optics* **6**(8), S675.
- [21] Corbitt, T., D. Ottaway, E. Innerhofer, J. Pelc, and N. Mavalvala, 2006, *Phys. Rev. A* **74**, 21802.
- [22] Dahm, T., and D. J. Scalapino, 1997, *Journal of Applied Physics* **81**(4), 2002, URL <http://dx.doi.org/10.1063/1.364056>.
- [23] Farace, A., F. Ciccarello, R. Fazio, and V. Giovannetti, 2013, arXiv preprint arXiv:1306.1142 .
- [24] Fong, K. Y., L. Fan, L. Jiang, X. Han, and H. X. Tang, 2014, arXiv:1404.3427 .
- [25] Galland, C., N. Sangouard, N. Piro, N. Gisin, , and T. J. Kippenberg, 2013, arXiv:1312.4303 .
- [26] Genes, C., D. Vitali, P. Tombesi, S. Gigan, and M. Aspelmeyer, 2008, *Phys. Rev. A* **77**, 033804.
- [27] Gigan, S., H. R. Böhm, M. Paternostro, F. Blaser, J. B. Hertzberg, K. C. Schwab, D. Bauerle, M. Aspelmeyer, and A. Zeilinger, 2006, *Nature* **444**, 67.
- [28] Girvin, S., 2009, *Physics* **2**, 40.
- [29] Gröblacher, S., J. T. Hill, A. H. Safavi-Naeini, J. Chan, and O. Painter, 2013, *Applied Physics Letters* **103**(18), 181104, URL <http://scitation.aip.org/content/aip/journal/apl/103/18/10.1063/1.4826924>.
- [30] Gröblacher, S., J. Hertzberg, M. Vanner, G. Cole, S. Gigan, K. Schwab, and M. Aspelmeyer, 2009, *Nature Physics* **5**(7), 485.
- [31] Hane, K., and K. Suzuki, 1996, *Sensors and Actuators A: Physical* **51**, 179.
- [32] He, Q., and M. Reid, 2013, *Physical Review A* **88**(5), 052121.
- [33] Holmes, C. A., C. P. Meaney, and G. J. Milburn, 2012, *Phys. Rev. E* **85**, 066203, URL <http://link.aps.org/doi/10.1103/PhysRevE.85.066203>.
- [34] Hossein-Zadeh, M., and K. J. Vahala, 2010, *IEEE J. Sel. Top. Quantum Electron.* **16**(1), 276.
- [35] I. Favero, C. M., S. Camerer, D. König, H. Lorenz, J. P. Kotthaus, and K. Karrai, 2007, *Appl. Phys. Lett.* **90**, 104101.
- [36] Jaecklin, V., C. Linder, J. Brugger, N. de Rooij, J.-M. Moret, and R. Vuilleumier, 1994, *Sensors and Actuators A: Physical* **43**, 269 , ISSN 0924-4247, URL <http://www.sciencedirect.com/science/article/pii/0924424793006995>.
- [37] Jayich, A. M., J. C. Sankey, B. M. Zwickl, C. Yang, J. D. Thompson, S. M. Girvin, A. A. Clerk, F. Marquardt, and J. G. E. Harris, 2008, *New J. Phys.* **10**, 095008.
- [38] Jiang, C., Y. Cui, H. Liu, and G. Chen, 2014, arXiv:1404.3928 .
- [39] Jourdan, G., F. Comin, and J. Chevrier, 2008, *Phys. Rev. Lett.* **101**, 133904.
- [40] Karuza, M., C. Biancofiore, M. Bawaj, C. Molinelli, M. Galassi, R. Natali, P. Tombesi, G. Di Giuseppe, and D. Vitali, 2013, *Physical Review A* **88**(1), 013804, URL <http://dx.doi.org/10.1103/PhysRevA.88.013804>.
- [41] Kiesewetter, S., Q. He, P. Drummond, and M. Reid, 2013, arXiv preprint arXiv:1312.6474 .
- [42] Kim, K., and S. Lee, 2002, *J. Appl. Phys.* **91**, 4715.
- [43] Kimble, H. J., Y. Levin, A. B. Matsko, K. S. Thorne, and S. P. Vyatchanin, 2001, *Phys. Rev. D* **65**, 022002.
- [44] Kippenberg, T. J., and K. J. Vahala, 2008, *Science* **321**(5893), 1172.
- [45] Kleckner, D., and D. Bouwmeester, 2006, *Nature* **444**, 75.
- [46] Larson, J., and M. Horsdal, 2011, *Phys. Rev. A* **84**, 021804, URL <http://link.aps.org/doi/10.1103/PhysRevA.84.021804>.
- [47] Liberato, S. D., N. Lambert, and F. Nori, 2010, arXiv:1011.6295 , 1011.62951011.6295.
- [48] Lörch, N., J. Qian, A. Clerk, F. Marquardt, and K. Hammerer, 2014, *Physical Review X* **4**(1), 011015.
- [49] Lrch, N., J. Qian, A. Clerk, F. Marquardt, and K. Hammerer, 2014, *Phys. Rev. X* **4**, 011015, URL <http://link.aps.org/doi/10.1103/PhysRevX.4.011015>.
- [50] Marino, F., and F. Marin, 2010, arXiv:1006.3509 , 1006.3509.
- [51] Marquardt, F., and S. Girvin, 2009, arXiv preprint arXiv:0905.0566 .
- [52] Marquardt, F., J. G. E. Harris, and S. M. Girvin, 2006, *Phys. Rev. Lett.* **96**, 103901.
- [53] Meaney, C. P., R. H. McKenzie, and G. J. Milburn, 2011, *Phys. Rev. E* **83**, 056202, URL <http://link.aps.org/doi/10.1103/PhysRevE.83.056202>.
- [54] Metzger, C., M. Ludwig, C. Neuenhahn, A. Ortlieb, I. Favero, K. Karrai, and F. Marquardt, 2008, *Phys. Rev. Lett.* **101**, 133903.
- [55] Metzger, C. H., and K. Karrai, 2004, *Nature* **432**, 1002.
- [56] Nation, P. D., M. P. Blencowe, and E. Buks, 2008, *Phys. Rev. B* **78**, 104516.
- [57] Nichols, E. F., and G. F. Hull, 1901, *Phys. Rev. (Series I)* **13**, 307, URL <http://link.aps.org/doi/10.1103/PhysRevSeriesI.13.307>.

- [58] OConnell, A. D., M. Hofheinz, M. Ansmann, R. C. Bialczak, M. Lenander, E. L. M. Neeley, D. Sank, H. Wang, M. Weides, J. Wenner, J. M. Martinis, and A. N. Cleland, 2010, *Nature* **464**, 697.
- [59] Ojanen, T., and K. Borkje, 2014, arXiv:1402.6929 .
- [60] Palomaki, T., J. Teufel, R. Simmonds, and K. Lehnert, 2013, *Science* **342**(6159), 710.
- [61] Paternostro, M., S. Gigan, M. S. Kim, F. Blaser, H. R. Böhm, and M. Aspelmeyer, 2006, *New J. Phys.* **8**, 107.
- [62] Pikovski, I., M. R. Vanner, M. Aspelmeyer, M. Kim, and Č. Brukner, 2012, *Nature Physics* **8**(5), 393.
- [63] Poot, M., and H. S. van der Zant, 2012, *Phys. Rep.* **511**, 273.
- [64] Pozar, D. M., 1998, *Microwave Engineering* (John Wiley and sons).
- [65] Qian, J., A. Clerk, K. Hammerer, and F. Marquardt, 2011, arXiv preprint arXiv:1112.6200 .
- [66] Regal, C., J. Teufel, and K. Lehnert, 2008, *Nature Physics* **4**(7), 555.
- [67] Restrepo, J., J. Gabelli, C. Ciuti, and I. Favero, 2011, *Comptes Rendus Physique* **12**, 1011.3911.
- [68] Rodrigues, D. A., and A. D. Armour, 2010, *Phys. Rev. Lett.* **104**, 053601, URL <http://link.aps.org/doi/10.1103/PhysRevLett.104.053601>.
- [69] Russel, A., 1922, *Proc. Phys. Soc. London* **35**, 10.
- [70] Safavi-Naeini, A. H., T. P. M. Alegre, J. Chan, M. Eichenfield, M. Winger, Q. Lin, J. T. Hill, D. E. Chang, and O. Painter, 2011, *Nature* **472**(7341), 69, URL <http://dx.doi.org/10.1038/nature09933>.
- [71] Schliesser, A., O. Arcizet, R. Rivière, G. Anetsberger, and T. Kippenberg, 2009, *Nature Physics* **5**(7), 509.
- [72] Schliesser, A., P. DelHaye, N. Nooshi, K. J. Vahala, and T. J. Kippenberg, 2006, *Phys. Rev. Lett.* **97**, 243905.
- [73] Schliesser, A., R. Riviere, G. Anetsberger, O. Arcizet, and T. J. Kippenberg, 2008, *Nat. Phys.* **4**, 415.
- [74] Suchoi, O., B. Abdo, E. Segev, O. Shtempluck, M. Blencowe, and E. Buks, 2010, *Phys. Rev. B* **81**, 174525.
- [75] Teufel, J., T. Donner, D. Li, J. Harlow, M. Allman, K. Cicak, A. Sirois, J. Whittaker, K. Lehnert, and R. Simmonds, 2011, *Nature* **475**(7356), 359.
- [76] Teufel, J., D. Li, M. Allman, K. Cicak, A. Sirois, J. Whittaker, and R. Simmonds, 2011, *Nature* **471**(7337), 204.
- [77] Teufel, J. D., D. Li, M. S. Allman, K. Cicak, A. J. Sirois, J. D. Whittaker, and R. W. Simmonds, 2010, arXiv:1011.3067 , 1011.3067.
- [78] Tholen, E. A., A. Ergul, E. M. Doherty, F. M. Weber, F. Gregis, and D. B. Haviland, 2007, *Appl. Phys. Lett.* **90**, 253509.
- [79] Thompson, J., B. Zwickl, A. Jayich, F. Marquardt, S. Girvin, and J. Harris, 2008, *Nature* **452**(7183), 72.
- [80] Walter, S., A. Nunnenkamp, and C. Bruder, 2013, arXiv preprint arXiv:1307.7044 .
- [81] Weinstein, A. J., C. U. Lei, E. E. Wollman, J. Suh, A. Metelmann, A. A. Clerk, and K. C. Schwab, 2014, arXiv:1404.3242 .
- [82] Weis, S., R. Riviere, S. Deleglise, E. Gavartin, O. Arcizet, A. Schliesser, and T. J. Kippenberg, 2010, *Science* **330**(6010), 1520, URL <http://dx.doi.org/10.1126/science.1195596>.
- [83] Xu, X., M. Gullans, and J. M. Taylor, 2014, arXiv:1404.3726 .
- [84] Xu, X.-W., H. Wang, J. Zhang, and Y.-x. Liu, 2013, *Phys. Rev. A* **88**, 063819, URL <http://link.aps.org/doi/10.1103/PhysRevA.88.063819>.
- [85] Yurke, B., and E. Buks, 2006, *J. Lightwave Tech.* **24**, 5054.
- [86] Zaitsev, S., O. Gottlieb, and E. Buks, 2012, *Nonlinear Dyn.* **69**, 1589.
- [87] Zaitsev, S., A. K. Pandey, O. Shtempluck, and E. Buks, 2011, *Phys. Rev. E* **84**, 046605, URL <http://link.aps.org/doi/10.1103/PhysRevE.84.046605>.
- [88] Zaitsev, S., A. K. Pandey, O. Shtempluck, and E. Buks, 2011, *Phys. Rev. E* **84**, 046605.
- [89] Zhou, X., F. Hocke, A. Schliesser, A. Marx, H. Huebl, R. Gross, and T. J. Kippenberg, 2013, *Nature Physics* **9**(3), 179, URL <http://dx.doi.org/10.1038/nphys2527>.